Catalysis Science & Technology

Accepted Manuscript

ROYAL SOCIETY OF CHEMISTRY

www.rsc.org/catalysis

Catalysis Science and Technology

COMMUNICATION

Water splitting reaction on $Ce_{0.15}Zr_{0.85}O_2$ driven by surface heterogeneity

Received 00th January 20xx,
Accepted 00th January 20xx

DOI: 10.1039/x0xx00000x

www.rsc.org/

Alfonsina Pappacena,[a] Marta Boaro,[a]† Lidia Armelao,[b] Llorca Jordi[c] and Alessandro Trovarelli[a]

$Ce_{0.15}Zr_{0.85}O_2$ was investigated in the two-step water splitting reaction. High temperature treatment in N_2 induced compositional and structural heterogeneities which contributed to a six-fold increase of H_2 yield after the first cycle. Ceria surface enrichment and the formation of a ceria-zirconia oxynitride phase positively affected the reduction and oxidation steps.

Solar thermochemical water splitting cycles (WSC) are an attractive carbon-free approach to H_2 production from water and sunlight.[1] Two-step metal oxide based cycles generate H_2 through high temperature (~1500-2000 °C) reduction in inert atmosphere and the subsequent water oxidation at an inferior (~400-1300 °C) temperature, making water splitting (WS) possible at lower temperatures than the thermodynamic value (2300 °C).[2] Among many metal oxides investigated in literature, ceria is one of the most viable candidates,[3] and it can deliver pure oxygen and hydrogen according to the following two-step redox cycle [4]

$$CeO_2\,(s) \rightarrow CeO_{2-\delta}\,(s) + \delta/2\ O_2 \quad \text{(endothermic step, T > 1800 °C)} \qquad (1)$$

$$CeO_{2-\delta}\,(s) + \delta H_2O\,(g) \rightarrow CeO_2\,(s) + \delta H_2\,(g) \quad \text{(exothermic step, 400-500 °C)} \qquad (2)$$

The main drawback of this cycle is that a significant reduction of ceria occurs only at temperatures higher than 1800 °C, where sublimation can occur with a decrease of the yield over cycles.[5] It follows that studies on ceria-based systems have been focused on lowering the reduction temperature of the Ce^{4+}/Ce^{3+} redox couple, while maintaining the high reactivity of reduced Ce^{3+} species towards water.[3,6] The addition of high valence dopant cations, such as Zr,$^{4+}$ proved effective in increasing the thermodynamic driving force of CeO_2 reduction at lower temperatures,[7-9] and the effect of zirconium content in the two step water splitting reaction has been widely studied.[10-14] Its presence favors CeO_2 reduction under inert atmosphere at temperatures lower than 1500 °C preventing sublimation and the consequent yield loss; moreover, the increased oxygen storage capacity of ceria-zirconia positively affects O_2 yield. On the other hand, the H_2 productivity depends on the number of exposed surface redox sites, and thus on the textural, morphological and structural properties of these materials. It was reported that in these materials the kinetics of water splitting is often hampered by gas-solid diffusion limitations due to the simultaneous occurrence of sintering processes. Several efforts have been made to overcome this issue, and the change of the morphological and structural properties of the mixed oxides by introducing other dopants[15] or by using different synthesis approaches[11,16,17] was found to be beneficial. Ceria-rich compositions have generally a good structural stability at the operating temperatures of the reduction step, while zirconia-rich compositions (Zr ≥ 50 mol%) are thermodynamically unstable in such conditions and undergo structural changes and phase segregation.[18] For this reason the majority of studies on the water splitting reaction over ceria-zirconia solid solutions focused on compositions with a zirconia content in the range up to 70 mol%,[10-17] although it has been recently reported that the occurrence of compositional heterogeneities may have a beneficial effect on the H_2 production step.[11] With the aim of gaining insights into this latter aspect and of exploring the potential application of ZrO_2-rich compositions in the WS reaction, despite their thermodynamic instability, we investigate here the reactivity and structural transformations of $Ce_{0.15}Zr_{0.85}O_2$ in the reduction and oxidation step of the cycle. It is shown that the solid solution undergoes structural evolution and compositional changes during high temperature treatments, with phase segregation and the formation of a N-containing ZrO_2 rich phase. This specific structural and compositional heterogeneity is shown to be responsible for the promotion of the WS reaction in this system. These

[a] Dipartimento di Chimica, Fisica e Ambiente, Università degli Studi di Udine, via del Cotonificio 108, 33100 Udine, Italy
[b] IENI-CNR and INSTM, Dipartimento di Scienze Chimiche, Università di Padova, Via Marzolo 1, 35131 Padova, Italy
[c] Institut de Tècniques Energètiques and Centre for Research in Nanoengineering, Universitat Politècnica de Catalunya, Diagonal 647, 08028 Barcelona, Spain
† corresponding author: marta.boaro@uniud.it
Electronic Supplementary Information (ESI) available: See
DOI: 10.1039/x0xx00000x

findings allow a step forward in the understanding of the structure/activity relationship in CeO_2-ZrO_2 based oxides.

$Ce_{0.15}Zr_{0.85}O_2$ solid solution was prepared through a surfactant assisted approach.[19] Fig. 1a shows that the material crystallizes in a tetragonal phase (PDF # 88-2398), in agreement with its nominal stoichiometry. Textural and oxygen storage properties of the fresh sample are reported in the supplementary section. The fresh material was treated at 1300 °C for 4 hours under N_2 flow before of the catalytic tests, in order to simulate the aging process occurring over several endothermic steps. After ageing, the surface area of the sample dropped to a negligible value (~1 m^2/g) due to sintering, and significant structural transformations were detected following the XRD analysis. In addition to the tetragonal phase of composition $Ce_{0.15}Zr_{0.85}O_2$, the XRD profile of the aged sample (Fig. 1b) identified the presence of a cubic ceria-rich and a monoclinic zirconia-rich phase, originated from segregation of the starting composition. The transformations are in agreement with those predictable from the ceria-zirconia phase stability diagram that shows the co-existence of monoclinic, tetragonal and cubic phases at 1300 °C.[18] Rietveld analysis of the diffractogram permitted a more precise identification of these phases and the results related to their quantification are reported in Table 1.

The surface chemical composition of the catalyst was determined by XPS analysis (see Table 1 and ESI for details). The measured Zr/Ce atomic ratio is equal to 1.8, a value significantly lower than expected for the $Ce_{0.15}Zr_{0.85}O_2$ composition (i.e. 5.6) indicating that restructuring of the material with formation of different phases also leads to a substantial ceria enrichment of the surface. This can be explained by a preferential migration of segregated $Ce_{0.70}Zr_{0.30}O_2$ cubic phase to the surface or subsurface region of the material.

Table 1: Structural and surface compositional characterization obtained from XRD and XPS measurements.

	XRD			XPS
Samples	Phase Composition			Atomic ratio
	Tetragonal $Ce_{0.15}Zr_{0.85}O_2$	Monoclinic $Ce_{0.12}Zr_{0.88}O_2$	Cubic $Ce_{0.70}Zr_{0.30}O_2$	Zr/Ce
N_2-aged	89.8 ± 0.1	8.6 ±0.4	1.6 ± 0.1	~1.8
air-aged	88.3 ± 0.1	8.9 ± 0.5	2.8 ± 0.2	~1.8
cycled	93.1 ± 0.1	4.8 ± 0.6	2.1 ± 0.2	~2.1

The activity of the aged sample in the two-step water splitting cycle was investigated by keeping separated the endothermic and exothermic step. The endothermic reduction in N_2 flow was calculated from the weight loss recorded during 80min isothermal test at 1300 °C in a thermogravimetric analyzer. The total O_2 release was of 165 µmol/g, equivalent to 825 µmol/g-CeO_2. The value is comparable to that found for solid solutions richer in ceria,[16] and corresponds to a Ce^{3+}/Ce_{tot} reduction yield of 56% relative to the initial composition, which is the highest reduction degree ever obtained by ceria-

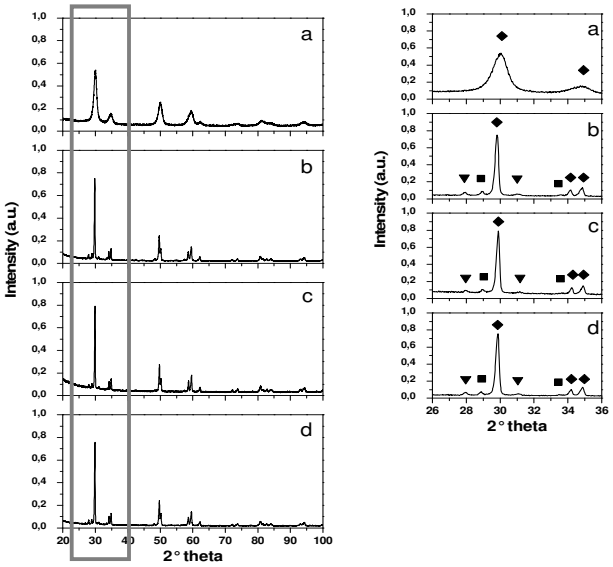

Fig. 1: X-ray diffractograms of catalyst: a) calcined at 500 °C, b) treated at 1300 °C in N_2 flow for 4h, c) treated at 1300 °C in air flow for 4h, and d) treated at 1300 °C in N_2 flow for 4h and tested over six redox cycles; ▼ monoclinic phase, ■ cubic phase, ◆ tetragonal phase.

zirconia oxides in this type of reaction. The high zirconia content of sample, coupled with a greater number of reducible sites exposed on its surface as the result of the ceria-rich phase segregation, can explain the present finding.

The exothermic oxidation of the catalyst with water vapor pulses was carried out at 800 °C in a gas analyzer by following an approach similar to that reported by Petkovich et al.[11] (see ESI for more details). Fig. 2 shows the results related to six H_2/H_2O redox cycles. H_2 production, as expected, was initially low (cycle 1), due to the thermodynamic and kinetic limitations[3,17] that hinder the reoxidation process in compositions containing a great quantity of zirconia with water. An interesting result, which triggered further investigations, was observed at the second redox cycle when a sharp increase in the reactivity was registered and remained nearly constant over the three subsequent cycles. At this stage, the H_2 yield (~100 µmoles/g) compares well with that found for most of the currently investigated ceria-zirconia compositions.[1]

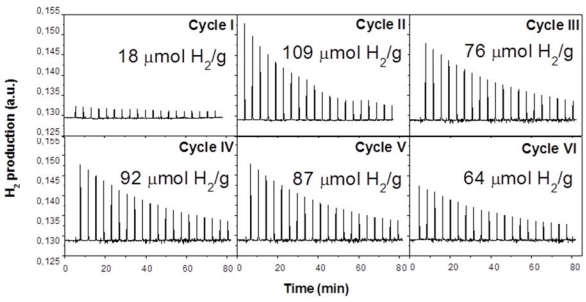

Fig. 2: H_2 production over six redox cycles at 800 °C of the sample treated in N_2 flow at 1300 °C for 4 hours.

In order to understand the role of the structural heterogeneity in the promotion effect of the redox behavior of the material, the sample was characterized at the atomic scale via HRTEM and XPS analysis, after aging and following the first two cycles.

Fig. 3A shows the HRTEM micrograph of the aged sample before the H_2/H_2O redox cycles. The inset shows that the sample was constituted by crystals from 5 up to 50 nm. Moreover, the analysis confirmed the presence of segregated phases at the nanoscale level. The area labeled "a" shows fringes at 3.0 Å corresponding to cubic CZ(111) planes related to surface segregated $Ce_{0.70}Zr_{0.30}O_2$. The figure shows also a representative lattice fringe image of the sample along with the Fourier Transform (FT) image corresponding to the area labeled "b". The FT pattern of this area is complex. The spot at 2.84 Å corresponds well to the (111) spacing of monoclinic $Ce_{0.12}Zr_{0.88}O_2$ phase. Spots at 2.61 Å could be ascribed to (020) planes of monoclinic ZrO_2. However, the spots at 5.22 Å, which are perfectly aligned with the (020) spots and exactly double the spacing at 2.61 Å, indicate that a supercell exists. Another example of this patterns is shown in the supporting information, Fig. S2. To the best of our knowledge no examples of superstructure can be found for monoclinic ZrO_2, while the formation of zirconia oxynitride superstructures was observed when zirconia powders were treated in N_2 at high temperature.[20] There is a very good correspondence between the (200) and (400) lattice fringes measured in the FT images at 5.1-5.2 and 2.5-2.6 Å, respectively, with those reported at 5.066 and 2.533 Å for Zr_2ON_2.[21] The slight differences could be due either to experimental errors or to the presence of Ce in the structure. Therefore, the FT can be attributed to a bixbyte-like Zr_2ON_2 structure, with possible inclusion of Ce atoms in the lattice, originated from the insertion of nitrogen into the lattice of zirconia-rich phases. XPS analysis (Fig. S5) supported the previous findings by revealing a weak, but significant N1s peak at BE energy of *ca*. 399 eV attributable to nitrogen in zyrconyl oxynitride phases.[22-24] Further confirmation of the existence of this phase was obtained by analysing the O1s peak (Fig. S6). The deconvolution of the O1s band showed a main component at 529.8 eV and a small shoulder at 531.5 eV which have been attributed to oxygen in the solid solution environment and in the zyrconil-oxynitride, respectively.[22]

HRTEM analysis of the sample after the second cycle showed that the zyrconil-oxynitride phase was stable and not disrupted by the water vapor oxidizing atmosphere. The micrograph in Fig. 3B clearly shows the presence of the oxynitride phase with the supercell spacings at 3.7 Å and 1.8 Å corresponding to the (220) and (440) crystallographic planes of the structure, respectively. Most of the oxynitride particles measure about 30-50 nm and are very crystalline.

In order to better disclose the role of the oxynitride phase in the production of H_2, we studied for comparison the behavior of a sample calcined in air for 4h at 1300 °C. Structural XRD data and surface XPS analysis reveal a situation nearly identical to that observed for the sample treated under N_2, Fig. 1c and Table 1. Fig. 4A shows a representative HRTEM image of this sample with lattice fringes at 3.0 and 1.5 Å corresponding to (111) and (222) crystallographic planes of the cubic $Ce_{0.7}Zr_{0.3}O_2$ phase.

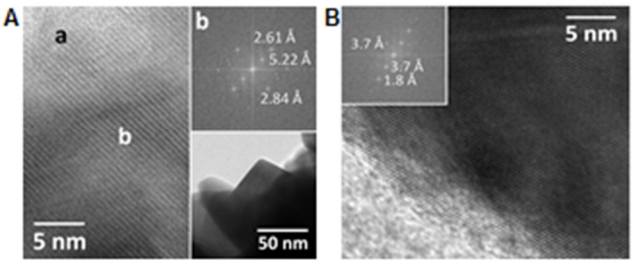

Fig. 3: A) HRTEM images of the sample treated in N_2 flow at 1300 °C for 4 hours, before testing; B) HRTEM image of sample treated in N_2 flow at 1300 °C for 4 hours and tested in water splitting conditions for two cycles (reduction in 5%H_2 in Ar at 800 °C, oxidation at 800 °C with 30% water vapor in He).

At the nanoscale level the catalyst was constituted only by ceria-zirconia crystallites of different structures, and no traces of the presence of oxynitride phase were detected.

In comparison to the catalyst aged under N_2, the air treated catalyst showed a lower initial H_2 yield (9 *vs.* 18 µmol/g) and a limited promotional effect (28 *vs.* 109 µmol/g), Fig. S7. It turned out that the existence at the nanoscale of the oxynitride phase might have a promotional positive effect on the water splitting reaction mechanism. This promotional effect can be originated from a good electronic-ionic mixed conductivity of Zr_2ON_2 phase under our operating conditions, which is known to positively affect the water splitting reaction.[25] The insertion of nitrogen in zirconia-rich structures to form a ceria-doped Zr_2ON_2-like phase brings in fact to the formation of vacancies which, depending on temperature and amount of nitrogen, can be randomly oriented or ordered.[26] In addition, nitrogen insertion into the ZrO_2 lattice modifies the electronic structure of the oxide.[27] The oxynitride phase can also constitute an intrinsic source of vacancies and highly active sites for the adsorption and activation of water, thanks to the presence of cerium as dopant.

On the other hand, this phase is present only at the surface at low concentration. Considering that the nature of the segregated phases and the surface characteristics of the material significantly influence the H_2 yield,[28] we can hypothesize that at the basis of the promotion there is a synergism among the phases. Water could be dissociatively adsorbed on the surface vacancies of the ceria-rich support and protons rapidly reduced thank to the cooperative effect of the oxynitride phase. The addition of nitrogen would contribute to modify acid-base properties of the surface, by increasing the basicity.[29] Basic sites along with oxygen vacancies have been shown to promote the H mobility,[30,31] and likely facilitating H recombination to form H_2. In this scheme, the oxynitride would play the role of a "catalytic center" contributing to accelerate charge and H transfer. From another standpoint, the oxynitride phase can constitute by itself an intrinsic source of vacancies[26], that cause surface rearrangements towards a configuration of vacancies and redox centers more suitable for WS reaction. Defects reorganization related to this phase may also justify the difference in promotion shown over redox cycles between N_2 and air treated samples. During cycling conditions an

increment in H_2 production was observed despite the presence of the oxynitride phase. In this case, compositional/structural heterogeneity might favor the nucleation at the nanoscale of more active ceria-zirconia redox centers[32,33] and oxynitride would contribute to catalyze these transformations. Further investigations are planned to properly understand the mechanism of water oxidation and the interactions between the involved phases.

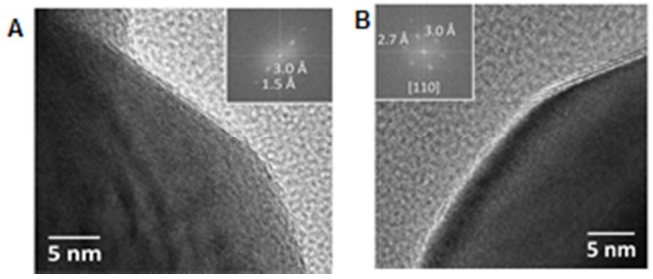

Fig. 4: HRTEM images of sample treated in air flow at 1300 °C for 4 hours; A) before testing, B) after two cycles, image of a CZ particle oriented along the [110] crystallographic direction.

Finally, it is worth noting that only a slight decrease of activity was evidenced starting from the last cycle. XPS analysis of the sample after this cycle (Fig. S6) evidenced that the zirconium oxynitride phase is still present, but an increase of the Zr/Ce ratio to a value of 2.1 was observed, Table 1. The corresponding X-ray powder diffractogram showed a slight redistribution among monoclinic, tetragonal and cubic phases (Table 1 and Fig. 1d) and conversely, HRTEM did not reveal the presence of any segregated phase (Fig. S3).

The results prove that in our specific conditions of testing agglomeration and phase reorganization processes occurred, causing a decrease in cerium content on the surface, that might explain the little deactivation observed. Additional studies, which go beyond the scope of this study, are required to ascertain the stability of this material in real two step water splitting operating conditions.

Conclusions

A ceria-zirconia oxide with a high amount of Zr (85 mol%) was tested in order to evaluate its potential use in the two-steps water splitting cycle for H_2 production. The typical temperature adopted in the endothermic step of the cycle induced structural changes with an enrichment in ceria of the surface and an unprecedented formation of a Zr_2ON_2 like-phase. These transformations resulted beneficial in both the reduction and oxidation steps. Moreover, redox cycles were found to promote H_2 production. All these findings favourably correlate surface and structural heterogeneity of ceria-zirconia to the increase in hydrogen production after cycling. It is suggested that redox cycling and presence of compositional heterogeneity at a nanoscale level is a key driver in the selection of good candidates for this process.

Aknowledgments

L.A. gratefully acknowledges MIUR for financial support through FIRB *Riname* RBAP114AMK project. The Authors thank Dr. Aneggi Eleonora (University of Udine) for Rietveld refinement. J.L. is Serra Húnter Fellow and is grateful to ICREA Academia program and MINECO (ENE2012-36368).

Notes and references

1 Z. Wang, R.R. Roberts, G.F. Naterer, K.S. Gabriel, *Int. J. Hydrogen Energy,* 2012, **37**, 16287.
2 T. Kodama, N. Gokon, *Chemical Reviews,* 2007, **107**, 4048.
3 J.R. Scheffe, A. Steinfeld, *Mater. Today,* 2014, **17**, 341.
4 C.C. William, M. Sossina, A. Haile, *Phil. Trans. R. Soc. A,* 2010, **368**, 3269.
5 S. Abanades, G. Flamant, *Solar Energy,* 2006, **80**, 1611.
6 S.G. Rudisil, L.J. Venstrom, N.D. Petkovich, T. Quan, N. Hein, D.B. Boman, J.H. Davidson, A. Stein, *J. Phys. Chem C,* 2013, **117**, 1692.
7 T. Kim, J.M. Vohs, R.J. Gorte, *Ind. Eng. Chem. Res.,* 2006, **45**, 5561.
8 G. Zhou, P.R. Shah, T. Kim, P. Fornasiero, J.R. Gorte, *Catal. Today,* 2007, **123**, 86.
9 R. di Monte, J. Kaspar, *Catal. Today,* 2005**, 100**, 27.
10 A. Le Gal, S. Abanades, *Int. J. Hydrogen Energy,* 2011, **36**, 4739.
11 N.D. Petkovich, S.G. Rudisill, L.J. Venstrom, D.B. Boman, J.H. Davidson, A. Stein, *J. Phys. Chem. C,* 2011, **115**, 21022.
12 H. Kaneko, S. Taku, T. Tamaura, *Solar Energy,* 2011, **85**, 2321.
13 Y. Hao, C-K. Yang, M.H. Sossina, *Chem. Mat*., 2014**, 26**, 6073.
14 J.T. Jang, K.J. Yoon, J.W. Bae, G.Y. Han, *Solar Energy,* 2014**,** 70.
15 A. Le Gal and S**.** Abanades**,** *J. Phys. Chem. C,* 2012, **116**, 13516.
16 A. Le Gal, S. Abanades, N. Bion, T. Le Mercier and V. Harlé, *Energy Fuels* 2013, **27**, 6068.
17 A. Le Gal, S. Abanades, G. Flamant, *Energy Fuels,* 2011, **25**, 4836.
18 M. Yashima, H. Arashi, M. Kakihana, M. Yoshimura*, J. Am. Ceram. Soc.,* 1994, **77**, 1067.
19 A. Pappacena, K. Schermanz, A. Sagar, E. Aneggi, A. Trovarelli, *Stud. Surf. Sci. Catal.,* 2010**, 175**, 835.
20 M. Lerch, *J. Am. Ceram. Soc.,* 1996, **79**, 2641.
21 E. Füglein, R. Hock, M. Lerch, *Z. Anorg. Allg. Chem.,* 1997**, 623**, 304.
22 G.I. Cubillos, M. Bethencourt, J.J. Olaya, *Appl. Surf. Sci.,* 2015**, 327**, 288.
23 A. Rizzo, M.A. Signore, L. Mirenghi, L. Tapfer, E. Piscopiello, E. Salernitano, R. Giorgi, *Thin Solid Films,* 2012, **520**, 3532.
24 A. Rizzo, M.A. Signore, L. Mirenghi, E. Piscopiello, L. Tapfer, *J. Phys. D: Appl. Phys.,* 2009**, 42**, art 235401.
25 Q.-L. Meng, C.I. Lee, T. Ishihara, H. Kaneko, Y. Tamaura, *Int. J. Hydrogen Energy*, 2011, **36**, 13435.
26 S.J. Clarke, C.W. Michie, M.J. Rosseinsky, *J. Solid State Chem*., 1999, **146**, 399.
27 T. Mishima, M. Matsuda, M. Miyake, *Appl. Catal. A,* 2007, **324**, 77.
28 A. Pappacena, M. Boaro, O. Šolcová, A. Trovarelli, *Adv. Sci. Tech*., 2014, **93**, 76.
29 N. Fripiat, V. Parvulescu, V.I. Parvulescu, P. Grange, *Appl. Catal. A,* 1999, **181,** 331.
30 D. Martin, D. Duprez, *J. Phys. Chem. B,* 1997, **101**, 4428.
31 R.C. Rabelo Neto and M. Schmal, *Appl.Catal. A*, 2013, **450**, 131
32 M.P. Yeste, J.C. Hernandez-Garrido, D.C. Arias, G. Blanco, J.M. Rodriguez-Izquierdo, J.M. Pintado, S. Bernal, J.A. Perez Omil and J.J. Calvino, *J. Mater. Chem. A*, 2013, **1**, 4836.
33 R. Wang, P.A. Crozier, R. Sharma, *J. Mater Chem*., 2010**, 20**, 7497.